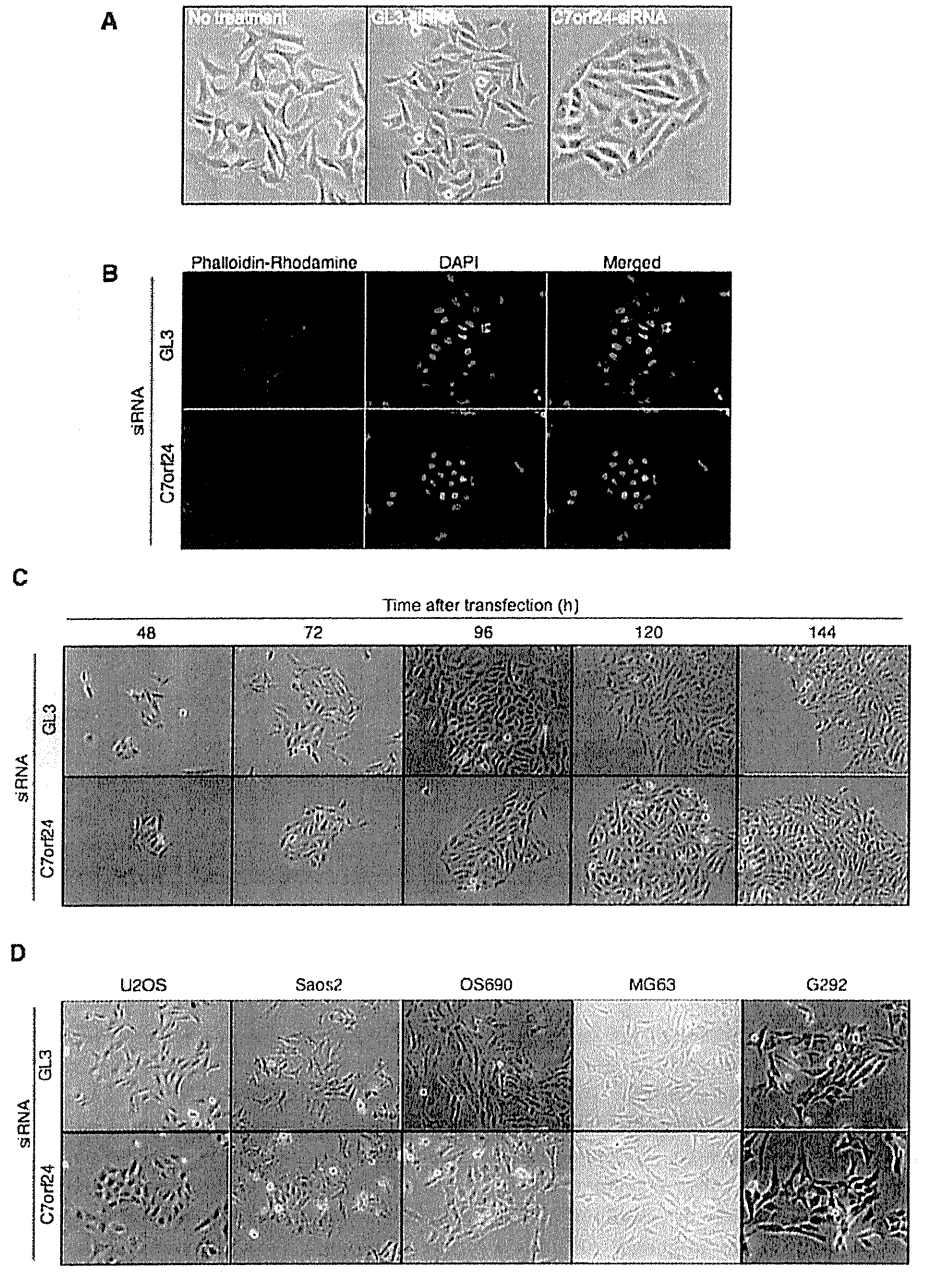

Figure 4. *Morphological changes of OS cells treated with C7orf24-siRNA. A: Phase-contrast micrographs of HOS 72 h after the transfection of siRNAs (10 nM). B: Fluorescent micrographs of HOS 72 h after the transfection of siRNAs (10 nM). C: Phase-contrast micrographs of HOS cells treated with siRNSs (10 nM) for the period indicated. D: Phase-contrast micrographs of OS cell lines 72 h after the transfection of siRNAs (10 nM).*

cancer/normal whole-genome microarray data sets to form an integrated training data set with 799 samples from 21 tissue types, not including bone sarcomas (17). Here we demonstrated that *C7orf24* expression is also up-regulated in bone sarcomas.

Oakley *et al.* tried to purify human γ-glutamyl cyclotransferase (GGCT) (18), an enzyme in the γ-glutamyl cycle that catalyzes the formation of 5-oxoproline from γ-glutamyl dipeptides and potentially plays a role in glutathione homeostasis (19, 20). They found that the gene

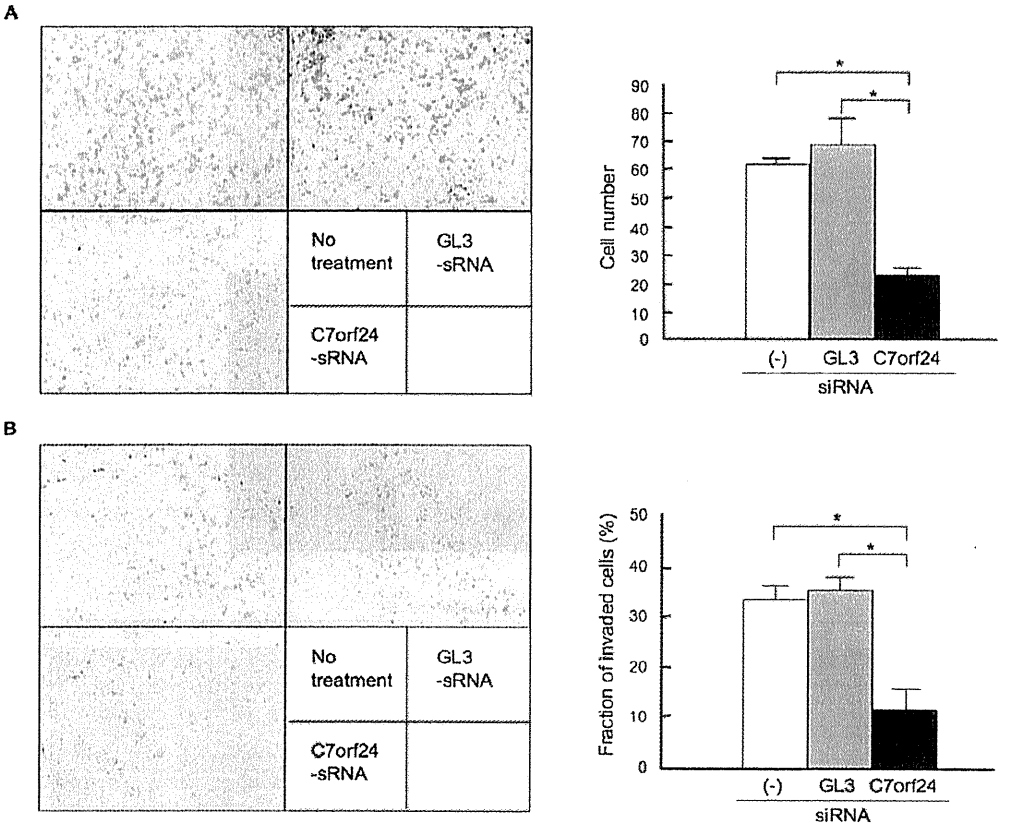

Figure 5. *Motility and invasiveness of HOS cells treated with siRNAs. A: Motility of HOS cells. Cells that passed through the pore of the control membrane were stained (left panel) and the positively stained cells were counted (right panel). B: Invasiveness of HOS cells. Cells that passed through the matrigel were stained (left panel) and the positive by stained cells were counted. The fraction of invading cells was determined as described in Materials and Methods and is indicated in the right panel.*

encoding GGCT is *C7orf24* (18), although the functional relevance to the growth of cancer cells is not known. Recently, Gromov *et al.* identified C7orf24 as an up-regulated protein by 2DE proteomic analyses in 123 samples of breast cancer (21). They validated the up-regulation of C7orf24 expression using a larger number of samples (2,197 samples) and found that approximately one fourth of tumors expressed C7orf24. Interestingly, the prognosis was poorer for patients with C7orf24-positive tumors than those with C7orf24-negative tumors. They also analyzed other types of cancer, including cervical, lung and colon cancer, and found that a significant proportion expressed C7orf24 (58%, 38%, and 72%, respectively). In addition, they established a method to monitor the level of C7orf24 in serum, and proposed C7orf24 as a general cancer biomarker.

In this study, we demonstrated that the knock-down of *C7orf24* expression inhibited the growth of OS cells, as we previously observed for bladder cancer cell lines. The molecular mechanism responsible for this inhibition is not yet known. Although the knockdown effect of *C7orf24*-siRNA showed no significant differences, the growth-inhibitory effect differed among cell lines. On treatment with *C7orf24*-siRNA, significant morphological changes were observed in HOS and, to a lesser degree, in other OS cell lines. Because the extent of the morphological change seemed to correspond to the degree of growth reduction in each cell line, these two phenotypes may be related to each other. In the case of HOS, the knockdown of *C7orf24* reduced cell motility and invasion, which also may relate to morphological changes. Based on these biological consequences, it is rational that gene ontology identified a set of genes related to cell adhesion as being up-regulated using *C7orf24*-siRNA. It is also intriguing that a set of genes relating to protein transport and localization was identified as being down-regulated using *C7orf24*-siRNA. Although we have no clear explanation of how these molecules contribute to the phenotype observed in this study, the current findings will be useful for understanding the role of C7orf24 in cancer.

Table I. *Genes up- or down-regulated by C7orf24-siRNA.*

Entrez gene number	Description	Ontological term	
		Cell adhesion	System development
Up-regulated genes			
780	Discoidin domain receptor family, member 1	+	
999	Cadherin 1, type 1, E cadherin (epithelial)	+	
1525	Coxsackie virus and adenovirus receptor	+	
1952	Cadherin, EGF LAG seven pass G type receptor 2 (flamingo homolog, Drosophila)	+	
3693	Integrin, beta 5	+	
3728	Junction plakoglobin	+	
4240	Milk fat globule EGF factor 8 protein	+	
4753	NEL-like 2 (chicken)	+	
4973	Oxidised low density lipoprotein (lectin-like) receptor 1	+	
10100	Tetraspanin 2	+	
10516	Fbulin 5	+	
50509	Collagen, type V, alpha 3	+	
130271	Pleckstrin homology domain containing, family H (with MyTH4 domain) member 2	+	
3730	Kallmann syndrome 1 sequence	+	+
3897	L1 cell adhesion molecule	+	+
7057	Thrombospondin 1	+	+
5376	Peripheral myelin protein 22		+
8522	Growth arrest specific 7		+
9241	Noggin		+
9723	Sema domain, immunoglobulin domain, short basic domain, secreted, (semaphorin) 3E		+
11075	Stathmin like 2		+
50861	Stathmin like 3		+
84612	Par 6 partitioning defective 6 homolog beta (*C. elegans*)		+

Entrez gene number	Description	Ontological term	
		Intracellular protein transport	Protein localization
Down-regulated genes			
5192	Peroxisome biogenesis factor 10	+	+
5824	Peroxisomal biogenesis factor 19	+	+
6747	Signal sequence receptor, gamma (translocon-associated protein gamma)	+	+
9590	A kinase (PRKA) anchor protein (gravin) 12	+	+
10254	Signal transducing adaptor molecule (SH3 domain and ITAM motif) 2	+	+
10802	SEC24 related gene family, member A (*S. cerevisiae*)	+	+
26985	Adaptor-related protein complex 3, mu 1 subunit	+	+
79716	Aminopeptidase like 1	+	+
89781	Hermansky Pudlak syndrome 4	+	+
130340	Adaptor-related protein complex 1, sigma 3 subunit	+	+
8934	RAB7, member RAS oncogene family like 1		+
51715	RAB23, member RAS oncogene family		+
54832	Vacuolar protein sorting 13 homolog C (*S. cerevisiae*)		+

Acknowledgements

We are grateful to Drs. Y. Shima, K. R. Shibata, K. Fukiage, and M. Furu for technical support. This work was supported by Grants-in-aid for Scientific Research from the Japan Society for the Promotion of Science, from the Ministry of Education, Culture, Sports, Science, and Technology, and from the Ministry of Health, Labor, and Welfare.

References

1 Nagarajan R, Clohisy D and Weigel B: New paradigms for therapy for osteosarcoma. Curr Oncol Rep *7*: 410-414, 2005.

2 Ferrari S, Smeland S, Mercuri M, Bertoni F, Longhi A, Ruggieri P, Alvegard TA, Picci P, Capanna R, Bernini G, Müller C, Tienghi A, Wiebe T, Comandone A, Böhling T, Del Prever AB, Brosjö O, Bacci G and Saeter G; Italian and Scandinavian

Sarcoma Groups: Neoadjuvant chemotherapy with high-dose Ifosfamide, high-dose methotrexate, cisplatin, and doxorubicin for patients with localized osteosarcoma of the extremity: a joint study by the Italian and Scandinavian Sarcoma Groups. J Clin Oncol *23*: 8845-8852, 2005.

3 Meyers PA, Schwartz CL, Krailo M, Kleinerman ES, Betcher D, Bernstein ML, Conrad E, Ferguson W, Gebhardt M, Goorin AM, Harris MB, Healey J, Huvos A, Link M, Montebello J, Nadel H, Nieder M, Sato J, Siegal G, Weiner M, Wells R, Wold L, Womer R and Grier H: Osteosarcoma: a randomized, prospective trial of the addition of ifosfamide and/or muramyl tripeptide to cisplatin, doxorubicin, and high-dose methotrexate. J Clin Oncol *23*: 2004-2011, 2005.

4 Goorin AM, Schwartzentruber DJ, Devidas M, Gebhardt MC, Ayala AG, Harris MB, Helman LJ, Grier HE and Link MP: Presurgical chemotherapy compared with immediate surgery and adjuvant chemotherapy for nonmetastatic osteosarcoma: Pediatric Onclogy Group Study POG-8651. J Clin Oncol *21*: 1574-1580, 2003.

5 DeLaney TF, Park L, Goldberg SI, Hug EB, Liebsch NJ, Munzenrider JE and Suit HD: Radiotherapy for local control of osteosarcoma. Int J Radiot Oncol Biol Phys *61*: 492-498, 2005.

6 Kim SY and Helman LJ: Strategies to explore new approaches in the investigation and treatment of osteosarcoma. Cancer Treat Res *152*: 517-528, 2009.

7 Khanna C, Wan X, Bose S, Cassaday R, Olomu O, Mendoza A, Yeung C, Gorlick R, Hewitt SM and Helman LJ: The membrane-cytoskeleton linker ezrin is necessary for osteosarcoma metastasis. Nat Med *10*: 182-186, 2004.

8 Maloney EK, McLaughlin JL, Dagdigian NE, Garrett LM, Connors KM, Zhou XM, Blättler WA, Chittenden T and Singh R: An anti-insulin-like growth factor I receptor antibody that is a potent inhibitor of cancer cell proliferation. Cancer Res *63*: 5073-5083, 2003.

9 Scotlandi K, Manara MC, Nicoletti G, Lollini PL, Lukas S, Benini S, Croci S, Perdichizzi S, Zambelli D, Serra M, García-Echeverría C, Hofmann F and Picci P: Antitumor activity of the insulin-like growth factor-I receptor kinase inhibitor NVP-AEW541 in musculoskeletal tumors. Cancer Res *65*: 3868-3876, 2005.

10 Kim SY, Lee CH, Midura BV, Yeung C, Mendoza A, Hong SH, Ren L, Wong D, Korz W, Merzouk A, Salari H, Zhang H, Hwang ST, Khanna C and Helman LJ: Inhibition of the CXCR4/CXCL12 chemokine pathway reduces the development of murine pulmonary metastases. Clin Exp Metastasis *25*: 201-211, 2008.

11 Morioka K, Tanikawa C, Ochi K, Daigo Y, Katagiri T, Kawano H, Kawaguchi H, Myoui A, Yoshikawa H, Naka N, Araki N, Kudawara I, Ieguchi M, Nakamura K, Nakamura Y and Matsuda K: Orphan receptor tyrosine kinase ROR2 as a potential therapeutic target for osteosarcoma. Cancer Sci *100*: 1227-1233, 2009.

12 Song B, Wang Y, Xi Y, Kudo K, Bruheim S, Botchkina GI, Gavin E, Wan Y, Formentini A, Kornmann M, Fodstad O and Ju J: Mechanism of chemoresistance mediated by miR-140 in human osteosarcoma and colon cancer cells. Oncogene *28*: 4065-4074, 2009.

13 Gougelet A, Pissaloux D, Besse A, Perez J, Duc A, Dutour A, Blay JY and Alberti L: miRNA profiles in osteosarcoma as a predictive tool for ifosfamide response. Int J Cancer 2010 [Epub ahead of print].

14 Kageyama S, Iwaki H, Inoue H, Isono T, Yuasa T, Nogawa M, Maekawa T, Ueda M, Kajita Y, Ogawa O, Toguchida J and Yoshiki T: A novel tumor-related protein, C7orf24, identified by proteome differential display of bladder urothelial carcinoma. Proteomics Clin Appl *1*: 192-199, 2007.

15 Masuda Y, Maeda S, Watanabe A, Sano Y, Aiuchi T, Nakajo S, Itabe H and Nakaya K: A novel 21-kDa cytochrome *c*-releasing factor is generated upon treatment of human leukemia U937 cells with geranylgeraniol. Biochem Biophys Res Commun *346*: 454-460, 2006.

16 Zhang C, Li HR, Fan JB, Wang-Rodriguez J, Downs T, Fu XD and Zhang MQ: Profiling alternatively spliced mRNA isoforms for prostate cancer classification. BMC Bioinformatics *7*: 202, 2006.

17 Xu L, Geman D and Winslow RL: Large-scale integration of cancer microarray data identifies a robust common cancer signature. BMC Bioinformatics *8*: 275, 2007.

18 Oakley AJ, Yamada T, Liu D, Coggan M, Clark AG and Board PG: The identification and structural characterization of C7orf24 as gamma-glutamyl cycl otransferase. An essential enzyme in the gamma-glutamyl cycle. J Biol Chem *283*: 22031-22042, 2008.

19 Orlowski M and Meister A: γ-Glutamyl cyclotransferase. Distribution, isozymic forms, and specificity. J Biol Chem *248*: 2836-2844, 1973.

20 Meister A and Anderson ME: Glutathione. Annu Rev Biochem *52*: 711-760, 1983.

21 Gromov P, Gromova I, Friis E, Timmermans-Wielenga V, Rank F, Simon R, Sauter G and Moreira JM: Proteomic profiling of mammary carcinomas identifies C7orf24, a gamma-glutamyl cyclotransferase, as a potential cancer biomarker. J Proteome Res *9*: 3941-3953, 2010.

Received December 19, 2010
Revised March 24, 2011
Accepted March 24, 2011

Oncogene (2011) 1–11

www.nature.com/onc

ORIGINAL ARTICLE

Identification of AFAP1L1 as a prognostic marker for spindle cell sarcomas

M Furu[1,2,11], Y Kajita[1,3,11], S Nagayama[4], T Ishibe[1,2], Y Shima[1,2], K Nishijo[1,2], D Uejima[1,5], R Takahashi[1,4], T Aoyama[1,5], T Nakayama[2], T Nakamura[2], Y Nakashima[6], M Ikegawa[7], S Imoto[8], T Katagiri[9,12], Y Nakamura[9] and J Toguchida[1,2,10]

[1]Department of Tissue Regeneration, Institute for Frontier Medical Sciences, Kyoto University, Kyoto, Japan; [2]Department of Orthopaedic Surgery, Graduate School of Medicine, Kyoto University, Kyoto, Japan; [3]Department of Urology, Graduate School of Medicine, Kyoto University, Kyoto, Japan; [4]Department of Surgery, Graduate School of Medicine, Kyoto University, Kyoto, Japan; [5]Department of Orthopaedic Surgery, Kansai Medical University, Osaka, Japan; [6]Department of Diagnostic Pathology, Kyoto University Hospital, Kyoto, Japan; [7]Department of Genomic Medical Sciences, Graduate School of Medical Science, Kyoto Prefectural University of Medicine, Kyoto, Japan; [8]Laboratory for DNA Information Analysis, Human Genome Center, Institute of Medical Science, The University of Tokyo, Kyoto, Japan; [9]Laboratory of Molecular Medicine, Human Genome Center, Institute of Medical Science, The University of Tokyo, Kyoto, Japan and [10]Center for iPS Cell Research and Application, Kyoto University, Kyoto, Japan

Spindle cell sarcomas consist of tumors with different biological features, of which distant metastasis is the most ominous sign for a poor prognosis. However, metastasis is difficult to predict on the basis of current histopathological analyses. We have identified actin filament-associated protein 1-like 1 (AFAP1L1) as a candidate for a metastasis-predicting marker from the gene expression profiles of 65 spindle cell sarcomas. A multivariate analysis determined that AFAP1L1 was an independent factor for predicting the occurrence of distant metastasis ($P=0.0001$), which was further confirmed in another set of 41 tumors by a quantitative mRNA expression analysis. Immunohistochemical staining using paraffin-embedded tumor tissues revealed that the metastasis-free rate was significantly better in tumors negative for AFAP1L1 ($P=0.0093$ by log-rank test). Knocking down the *AFAP1L1* gene in sarcoma cells resulted in inhibition of the cell invasion, and forced expression of AFAP1L1 in immortalized human mesenchymal stem cells induced anchorage-independent growth and increased cell invasiveness with high activity levels of matrix metallopeptidase. Furthermore, tumor growth *in vivo* was accelerated in AFAP1L1-transduced sarcoma cell lines. These results suggest that AFAP1L1 has a role in the progression of spindle cell sarcomas and is a prognostic biomarker.

Oncogene advance online publication, 25 April 2011; doi:10.1038/onc.2011.108

Keywords: AFAP1L1; spindle cell sarcoma; metastasis; prognostic marker

Correspondence: Professor J Toguchida, Institute for Frontier Medical Sciences, Kyoto University, 53 Kawahara-cho, Shogoin, Sakyo-ku, Kyoto 606-8507, Japan.
E-mail: togjun@frontier.kyoto-u.ac.jp
[11]These authors contributed equally to this work.
[12]Current address: Division of Genome Medicine, Institute for Genome Research, The University of Tokushima, Japan.
Received 27 October 2010; revised 11 February 2011; accepted 2 March 2011

Introduction

Sarcomas are non-epithelial malignant tumors that develop in mesenchymal tissue and classified into two groups on the basis of cellular morphology. Small round cell sarcomas, also known as blue tumors from their color on hematoxylin and eosin staining, include alveolar rhabdomyosarcomas and Ewing's sarcomas that develop in soft tissue and bone, respectively. Both have tumor-specific chromosomal translocations creating tumor-specific fusion genes (Helman and Meltzer, 2003; Toguchida and Nakayama, 2009). Spindle cell sarcomas, named for their flattened, elongated and fibroblastic morphology, far outnumber the first group. Malignant fibrous histiocytomas (MFHs) and ostesarcomas, the prototypes of this second group, develop in soft tissue and bone, respectively. They are generally radio- and chemoresistant, although high-dose, multidrug combination chemotherapy is effective for osteosarcomas. Except for some tumors, such as synovial sarcomas, which are characterized as having *SYT–SSX* fusion genes (Clark *et al.*, 1994), most spindle cell sarcomas lack tumor-specific genetic alterations (Toguchida and Nakayama, 2009). Mutations of tumor suppressor genes such as the *RB* and *p53* genes are found in many cases but not all (Toguchida *et al.*, 1992; Wadayama *et al.*, 1994). The histopathological complexity of soft tissue sarcomas is an issue. For example, MFH used to be considered the most prevalent soft tissue sarcoma but now the pathological concept is controversial (Fletcher *et al.*, 2001). To overcome this complexity, a number of gene expression profiling studies have been performed to classify spindle cell sarcomas and identify prognostic markers (Nielsen *et al.*, 2002; Lee *et al.*, 2004; Francis *et al.*, 2007; Nakayama *et al.*, 2007). Our group has also identified such markers using a custom-made cDNA microarray consisting of 23 040 genes in various types of malignant tumors (Nagayama *et al.*, 2002). As for synovial sarcomas, we have identified fibroblast growth factor (Ishibe *et al.*, 2005), Wnt-FZD10 (frizzled homolog 10) (Nagayama *et al.*, 2005) and retinoic acid

signals as molecular targets in synovial sarcomas (Ishibe *et al.*, 2008). For other types of tumors, however, the identification of tumor-specific markers is made difficult by small numbers of cases. Therefore, we have taken a different approach using the microarray data, trying to identify genes associated with aggressive phenotypes irrespective of the pathological diagnosis. Using distant metastasis as a discriminating factor, we have identified actin filament-associated protein 1-like 1 (AFAP1L1) as a candidate prognostic marker for spindle cell sarcomas. Here, we report that AFAP1L1 has a significant role in the progression of spindle cell sarcomas and is a prognostic marker as well as a potential target for molecular therapy.

Results

Identification of AFAP1L1 as a metastasis-related gene in spindle cell sarcomas

Genome-wide gene expression profiles of 65 soft tissue spindle cell sarcomas (STSs) were analyzed with a cDNA microarray system consisting of 23 040 genes, and mesenchymal stem cells (MSCs) were used as a reference (Nagayama *et al.*, 2002). The expression of each gene in tumor samples was demonstrated as the ratio of the signal intensity in tumor samples and MSCs (Nagayama *et al.*, 2002). Tumor samples were classified as positive for the gene if the ratio was more than 1.0, and negative if the ratio was 1.0 or less. Distant metastases developed in 29 cases, the remaining 36 patients being metastasis-free until the last follow-up (minimum of 61 months). The fraction of cases positive for each gene was calculated among tumors with and without metastasis, and statistical analyses were performed to identify genes associated with distant metastasis. This procedure identified the *AFAP1L1* gene, for which 21 of 29 cases with metastasis (Figure 1a) and 11 of 36 cases without metastasis (Figure 1b) were positive, and the difference was statistically significant ($P=0.0011$, Fisher's exact test). When the 65 cases were divided into AFAP1L1 (+) and AFAP1L1 (−) groups on the basis of the value relative to that of MSC, the metastasis-free fraction of AFAP1L1 (+) cases was lower than that of AFAP1L1 (−) cases (Figure 1c). AFAP1L1 is a member of the AFAP family along with AFAP-110 and AFAP1L2. AFAP-110 was identified as one of several major substrates of the viral oncogenic protein tyrosine kinase v-Src (Kanner *et al.*, 1990; Flynn *et al.*, 1993) and has been shown to function as an actin filament crosslinking protein with a fundamental role in the actin cytoskeleton's arrangement (Baisden *et al.*, 2001a). Moreover, it has been demonstrated that AFAP-110 is overexpressed in breast and prostate cancers and contributes to tumorigenic growth by regulating focal contact sites (Dorfleutner *et al.*, 2007; Zhang *et al.*, 2007). No previous reports concerning the function or involvement in cancer of AFAP1L1 have been published.

Although the overall amino-acid sequence similarity between AFAP-110 and AFAP1L1 is as much as 44%,

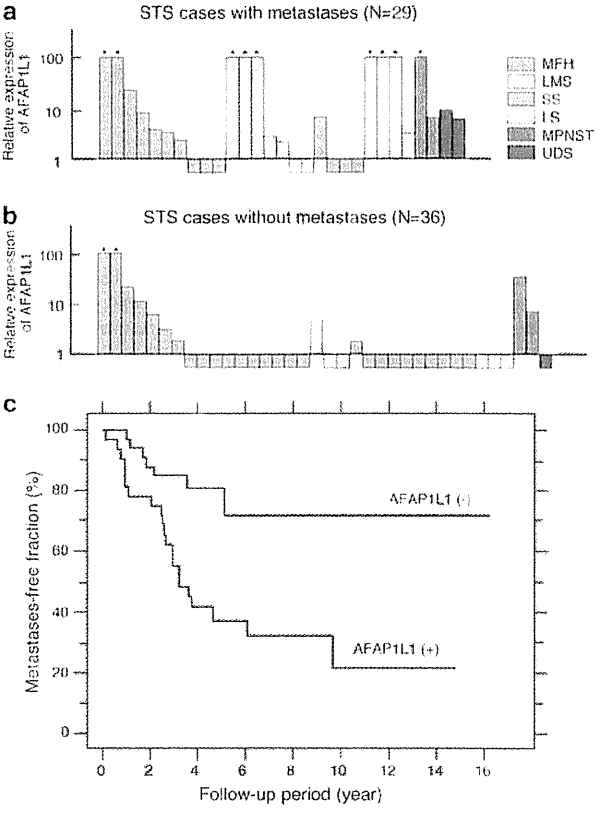

Figure 1 Identification of the *AFAP1L1* gene as a metastasis-associated gene of STSs. Expression of the *AFAP1L1* gene in STSs with metastasis ($N=29$) (**a**), and without metastasis ($N=36$) (**b**). The expression level of the *AFAP1L1* gene in each tumor is demonstrated relative to that in human bone marrow stem cells (hBMSCs). For convenience, the highest value is set as 100. Samples with a relative value of more than 100 are indicated by asterisks, and those with a relative value of less than 1.0, by rectangles. LMS, leiomyosarcoma; LS, liposarcoma; MFH, malignant fibrous histiocytoma; MPNST, malignant peripheral nerve sheath tumor; SS, synovial sarcoma; UDS, undifferentiated sarcoma. (**c**) Metastasis-free fraction of the initial set of STSs. A total of 65 STSs were divided by the expression level of the *AFAP1L1* gene relative to that in hBMSCs: the relative value in AFAP1L1 (+) tumors was more than 1.0 and the relative value in AFAP1L1 (−) tumors was equal to or less than 1.0. The metastasis-fee fraction of each group was demonstrated by a Kaplan–Meier curve.

AFAP1L1 shared most of the predicated domain structures with AFAP-110, such as two pleckstrin homology domains, two Src homology 2 domains (SH2), and a putative leucine zipper domain (Figure 2a) (Baisden *et al.*, 2001a). A polyclonal antibody was raised against its 79 N-terminal amino acids, which showed no homology with AFAP-110 (Figure 2a). Western blotting using this antibody showed a band with a molecular size of 90–100 kD in cell lines expressing the *AFAP1L1* gene (Figure 2b). When a set of sarcomas and human MSCs (hMSCs) were analyzed by quantitative PCR (qPCR), clear differences in the expression patterns between AFAP-110 and AFAP1L1 were found (Figure 2c). The expression of AFAP1L1 was much higher in sarcoma

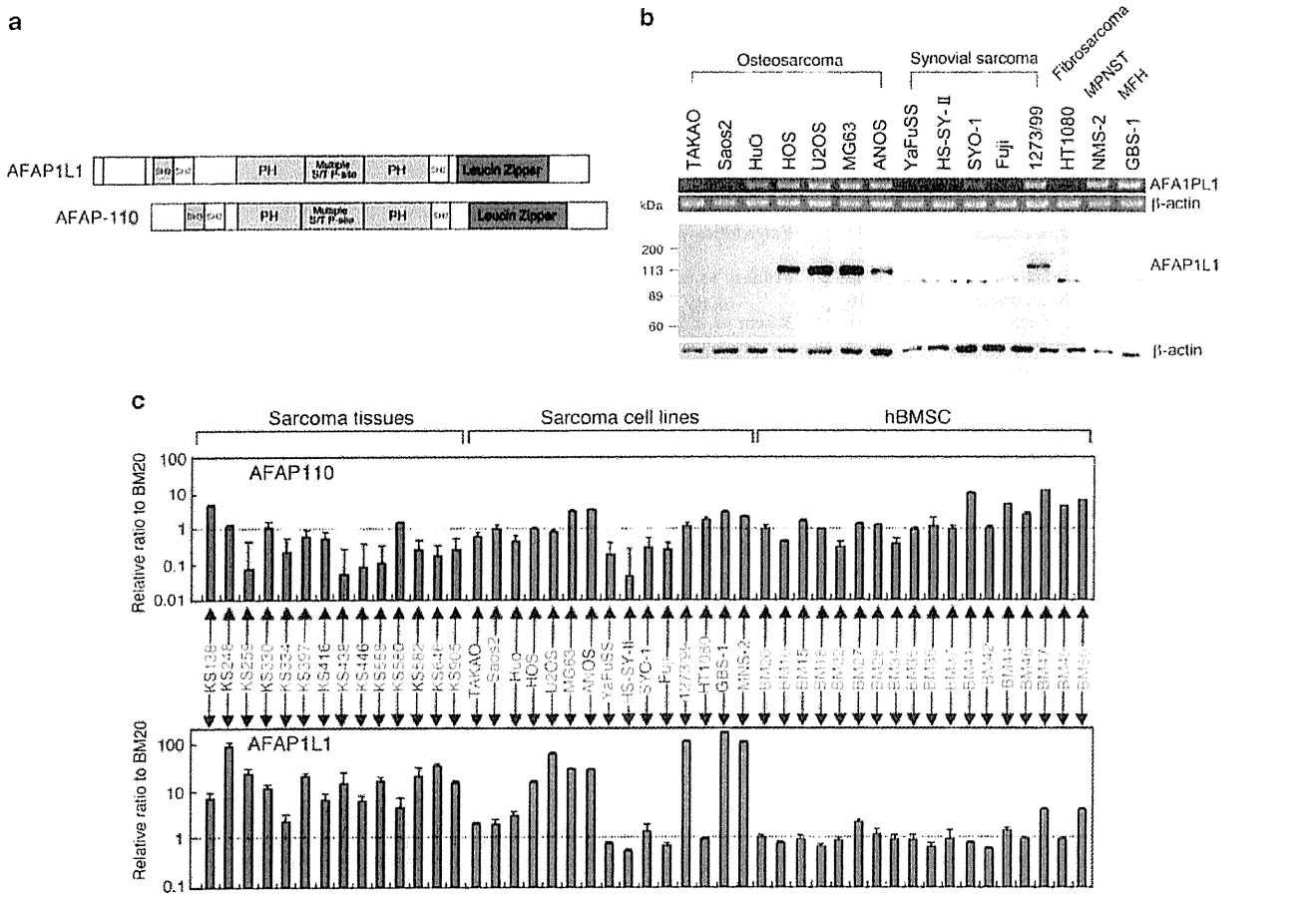

Figure 2 Comparison of AFAP-110 and AFAP1L1. (**a**) Predicted domain features of AFAP1L1 and AFAP-110. An oligopeptide derived from the hatched region was used as an antigen to raise a polyclonal antibody for APAP1L1.Validation of the anti-AFAP1L1 antibody. LZ, leucine zipper domain; PH, pleckstrin homology domain; SH2, Src homolog 2 motif. (**b**) Expression of AFAP1L1 in sarcoma cell lines. mRNA expression was analyzed by reverse transcription–PCR and protein expression was analyzed by western blotting using anti-AFAP1L1 antibody. β-Actin was used as a control. (**c**) Comparison of AFAP-110 and AFAP1L1 expression in cell lines and tissue samples. mRNA expression of AFAP-110 and AFAP1L1 in sarcoma tissues, sarcoma cell lines and human bone marrow stem cells (hBMSCs) was analyzed by qPCR. The expression level of each gene is demonstrated as a value relative to that in hBMSCs (BM20).

tissues and cell lines than in normal hMSCs ($P<0.0001$, Man–Whitney U test), whereas the expression of AFAP-110 was slightly higher in MSCs than in sarcoma tissues and cell lines ($P=0.0122$, Man–Whitney U test) (Figure 2c). On the basis of these results, we focused on the *AFAP1L1* gene.

Confirmation of the significance of AFAP1L1 in multivariate analyses

To confirm the significance of AFAP1L1 expression in the clinical behavior of STSs, the 65 cases were divided into two or more groups on the basis of clinicopathological factors, such as gender, age, location, size, depth, previous treatment history, surgery, and chemotherapy, pathological stage and pathological diagnosis, in addition to the expression of AFAP1L1 (Table 1). These factors were known to contribute to the prognoses in sarcoma patients (Ottaiano *et al.*, 2005). When the occurrence of distant metastases was used as an endpoint, AFAP1L1 expression was confirmed as a significant factor along with age and FNCLCC grade in univariate analyses (Table 1). These three factors were found to contribute independently to the prognosis in multivariate analyses (Table 1).

Association of AFAP1L1 expression with metastasis was confirmed in the second set of tumors

To confirm the significance of *AFAP1L1* gene expression, a second set of tumors consisting of 41 STSs was analyzed (Supplementary Table 1). Their clinical characteristics were almost equivalent to those of the tumors used in the initial analyses except for the pathological classification, due to a recent refinement of the diagnostic criteria for MFH (Fletcher *et al.*, 2002). STSs with no definitive features, which might be diagnosed as MFHs, were classified as 'undifferentiated sarcomas' in

Table 1 Cox's proportional hazards model analysis of factors relating to distant metastases in patients with STS

Variables	*Classes*	*No. of cases*	*Comparison*	*Hazard ratio*	*95% CI*	*Unfavorable/ Favorable*		P-*value*
Univariate analysis								
Gender	Female	39	Female vs male	0.872	0.416–1.828			0.7173
	Male	26						
Age	>60	31	≧60 vs <60	2.411	1.116–5.208	≧60	60>	0.0251
	<60	34						
Location	Extremities	44	Extremities vs trunk	0.759	0.350–1.645			0.4840
	Trunk	21						
History	Primary	49	Primary vs recurrence	1.212	0.517–2.843			0.6578
	Recurrence	16						
Size	>5 cm	51	≧5 cm vs <5 cm	1.787	0.620–5.154			0.2826
	<5 cm	14						
Depth	Superficial	24	Superficial vs deep	1.185	0.550–2.552			0.6640
	Deep	41						
FNCLCC	Grade 1	9	Grade 3 vs others	2.652	1.259–5.587	Grade 3	Grade 1 or 2	0.0103
	Grade 2	28						
	Grade 3	28						
Surgery	Wide	33	Wide vs others	0.954	0.460–1.981			0.9004
	Marginal	29						
	Intralesional	3						
Chemotherapy	Performed	29	Performed vs not performed	0.639	0.298–1.367			0.2482
	Not performed	36						
Diagnoses	MFH	27	MFH vs others	0.709	0.329–1.527			0.3795
	Synovial sarcoma	14						
	Leiomyosarcoma	10						
	Liposarcoma	7						
	MPNST	4						
	UDS	3						
AFAP1L1	Positive	32	Positive vs negative	3.611	1.592–8.195	Positive	Negative	0.0021
	Negative	33						
Multivariate analysis								
Age				2.908	1.069–7.907	≧60	60>	0.0365
FNCLCC				3.607	1.409–9.231	Stage 3	Stage 1 or 2	0.0075
AFAP1L1				4.001	1.656–9.665	Positive	Negative	0.0021

Abbreviations: AFAP1L1, actin filament-associated protein 1-like 1; CI, confidence interval; FNCLCC, Fédération Nationale des Centres de Lutte Contre le Cancer; MFH, malignant fibrous histiocytoma; MPNST, malignant peripheral nerve sheath tumor; STS, soft tissue spindle cell sarcoma; UDS, undifferetiated sarcoma.

most cases. During the follow-up period (4–210 months for all patients; 29–210 months for living patients), 18 developed distant metastases and 23 were free from metastasis until the last follow-up, and the qPCR analysis was used to evaluate the expression of the *AFAP1L1* gene in tumors of each group. In all, 48 of 65 samples in the first set of tumors were available for the qPCR analysis, which showed that the expression level of the *AFAP1L1* gene was significantly higher in tumors with metastasis ($N=29$) than without ($N=19$) ($P=0.0347$, Man–Whitney U test) (Figure 3a). A similar difference was found in the second set of tumors: The expression level of the *AFAP1L1* gene was significantly higher in tumors with metastasis ($N=23$) than without metastasis ($N=19$) ($P=0.0093$, Man–Whitney U test). Therefore, the association of *AFAP1L1* gene expression with metastatic activity was confirmed in the second set of STSs.

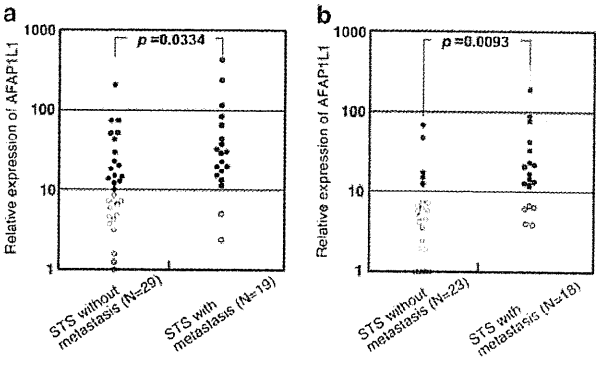

Figure 3 qPCR analyses of AFAP1L1 expression in STS. The expression level of the *AFAP1L1* gene in the first (**a**) and second (**b**) sets of STSs is demonstrated relative to that in human bone marrow stem cells.

Immunohistochemical analysis of AFAP1L1 protein in sarcomas

The expression of the AFAP1L1 protein was analyzed in paraffin-embedded specimens of 36 STSs from the second set of tumors, in which AFAP1L1 had already been analyzed by qPCR. On the basis of staining intensity of positive cells, tumors were classified into four groups; negative (−, 15 cases), weakly positive (+, 6 cases), moderately positive (++, 10 cases), and

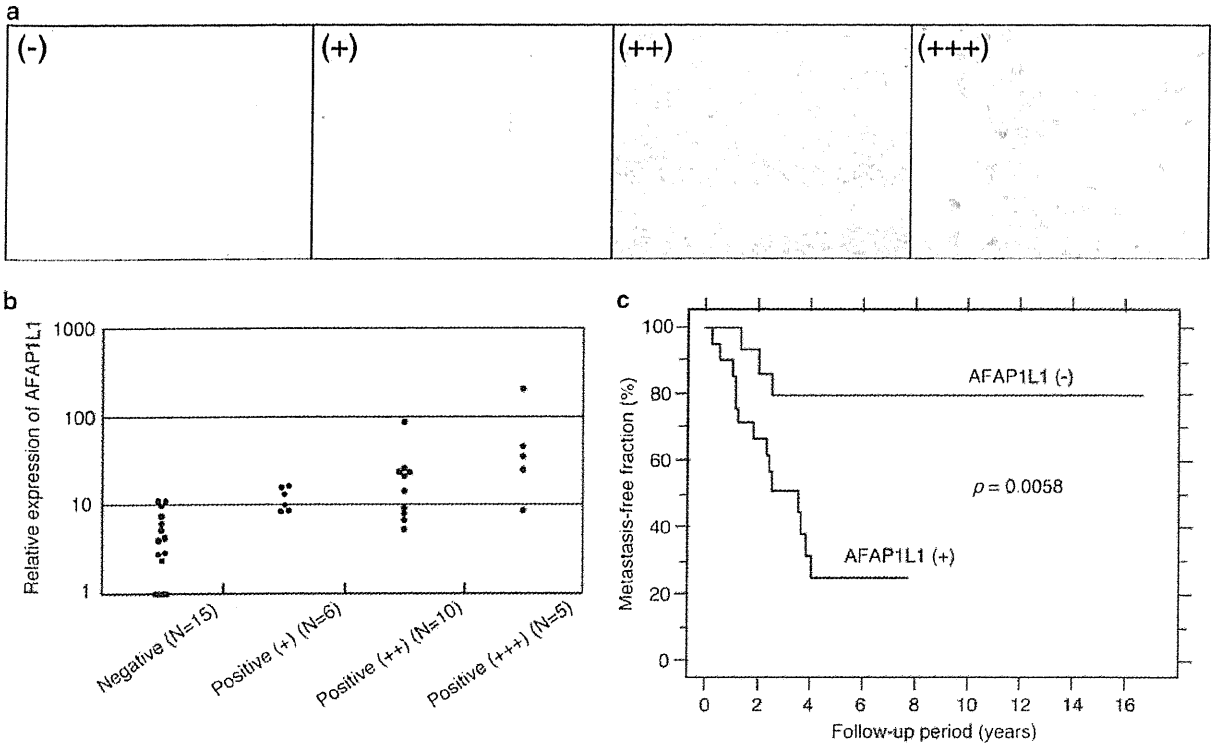

Figure 4 Expression of the AFAP1L1 protein in tumor tissues. (**a**) Expression of the AFAP1L1 protein in tumor tissues. Representative cases with negative (−), weak (+), moderate (+ +) or strong (+ + +) staining of AFAP1L1 are shown. (**b**) Relationship between the mRNA expression and immunostaining of AFAP1L1 in tumors. The mRNA level of the *AFAP1L1* gene in tumors used in the immunohistochemical analyses is demonstrated relative to that in human bone marrow stem cells. (**c**) Metastasis-free fraction of tumors with positive and negative staining of the AFAP1L1 protein. In all, 36 tumors were divided into AFAP1L1-negative (−; 15 cases) and -positive (+, + +, or + + +; 21 cases) groups, and the metastasis-fee fraction of each group was demonstrated by a Kaplan–Meier curve.

strongly positive (+ + +, 5 cases) (Figure 4a). The staining intensity of each tumor was consistent with the result of qPCR (Figure 4b). In positive cases, AFAP1L1 was detected predominantly in the cytoplasm of tumor cells. When tumors were simply divided into AFAP1L1-negative (−, 15 cases) and positive cases (+, + + and + + +, 21 cases), the stepwise regression model showed that the metastasis-free fraction of AFAP1L1-negative cases was significantly higher than that of positive cases (Figure 4c). There was no significant difference between tumors positive and negative for the staining in terms of patient's age, tumor size and tumor depth. As for FNCLCC grade, however, the number of high-grade tumor (grade 3) in positive cases (12/21 cases) was significantly higher than that in negative cases (3/15 cases) ($P = 0.0407$, Fisher's exact test). Therefore, the association of AFAP1L1 expression with metastasis was confirmed by both mRNA and protein analyses, suggesting AFAP1L1 to be a prognostic marker of spindle cell sarcomas.

Inhibition of AFAP1L1 expression reduced the invasiveness

We next generated AFAP1L1-knocked down cells to investigate the function of AFAP1L1 using an RNA interference system mediated by a lentivirus. U2OS and 1273/99 cells were used in these experiments because they had abundant AFAP1L1 expression among sarcoma cell lines tested (Figure 5a). Two non-targeting sequences for mammalian genes (control RNAi-1 and -2) and two AFAP1L1-targeting sequences (AFAP1L1 RNAi-1 and -2) were employed for further experiments. The transduction efficiency was 90–95% in U2OS cells and 85–90% in 1273/99 cells, as determined by counting EmGFP-positive cells (data not shown), and the knockdown of AFAP1L1 was confirmed effective by western blotting (Figure 5a). As for proliferative ability, no differences were found between the AFAP1L1-knockdown cells and control cells in the U2OS (Figure 5b) and 1273/99 cell lines (data not shown). However, matrigel invasion assays revealed that knocking down AFAP1L1 resulted in reduced cell invasiveness (Figure 5c).

Induction of AFAP1L1 gene expression conferred invasiveness

The cells of origin for sarcomas remain unclear but one possible candidate is the MSC (Matushansky *et al.*, 2007), so we chose immortalized human MSCs (ihMSCs) as a recipient for AFAP1L1 transduction. ihMSCs were established in our laboratory and shown to be fully transformed when the activated H-*ras* gene had been

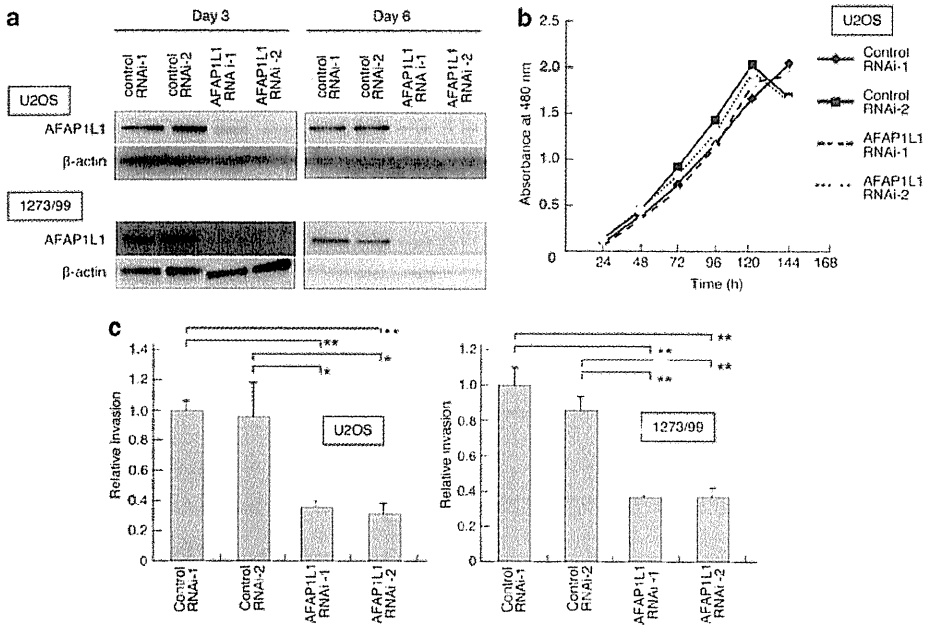

Figure 5 Downregulation of AFAP1L1 expression decreased invasiveness of sarcoma cells. (**a**) Western blotting of U2OS and 1273/99 cells transduced with microRNAs. Either non-targeting (control RNAi-1 or -2) or AFAP1L1-targeting (AFAP1L1 RNAi-1 or -2) microRNA was introduced and the expression of AFAP1L1 was analyzed 3 and 6 days later. (**b**) Growth curves of U2OS cells transduced with mircoRNAs. Cell viability was evaluated by WST-8 assay. (**c**) Invasive ability of U2OS and 1273/99 cells transduced with mircoRNAis. Matrix invasiveness was calculated as described in materials and methods, and demonstrated as fold change relative to control RNAi-1 cells. $^{**}P<0.01$; $^{*}P<0.05$.

introduced (Shima *et al.*, 2007). pLenti6/AFAP1L1 was transduced into ihMSCs, and several clones stably expressing AFAP1L1 were established (ihMSC/AFAP1L1) and used for further experiments (Figure 6a). The growth of AFAP1L1-transduced clones showed no significant change compared with that of the parental ihMSCs or ihMSC/LacZ cells (data not shown), whereas invasiveness and anchorage-independent growth were exaggerated in all four ihMSC/AFAP1L1 clones (Figures 6b and c).

Tumor invasiveness correlates with the activity of matrix metalloproteinases (MMPs), such as gelatinases, MMP-2 and MMP-9 (Egeblad and Werb, 2002; Overall and Kleifeld, 2006). To determine whether the increased invasive ability of the ihMSC/AFAP1L1 clones was related to increased excretion of MMPs, gelatin zymography was performed. The ihMSC/AFAP1L1 clones showed significantly increased activity of MMP-9 but not MMP-2 compared with control cells (Figure 6d). The increased excretion of MMP-9 in two ihMSC/AFAP1L1 clones was also confirmed by enzyme-linked immunosorbent assay (Figure 6e). These results suggest that AFAP1L1 endows ihMSCs with invasiveness, at least partly, by regulating MMP-9's excretion. In clinical samples, however, the expression level of MMP-9 was not clearly associated with that of AFAP1L1 ($R^2 = 0.248$) (Supplementary Figure S1).

Acceleration of tumor growth by AFAP1L1 expression in vivo

The inoculation of ihMSC/AFAP1L1 clones subcutaneously into immunodeficient mice produced no tumors (data not shown), indicating that the overexpression of AFAP1L1 in immortal cells was not enough for full transformation. To investigate whether AFAP1L1 modifies the phenotype of sarcoma cells without endogenous AFAP1L1 expression *in vivo*, stably expressing cell lines were generated using Saos2 cells as a recipient (Saos2/AFAP1L1) (Figure 7a). The growth of Saos2/AFAP1L1 clones *in vitro* showed no significant change compared with that of parental Saos2 or Saos2/LacZ control cells, but the invasive activity of Saos2/AFAP1L1 clones increased, which was consistent with that of ihMSC/AFAP1L1 clones (data not shown). These Saos2 clones were subcutaneously inoculated into the back of non-obese diabetic/severe combined immunodeficient mice to evaluate tumorigenesis and metastasis. Tumor growth was accelerated in Saos2/AFAP1L1 clones, although the extent of the increase seemed not to completely match the level of AFAP1L1 expression (Figures 7b and c). There was no metastasis by any Saos2/AFAP1L1 clones or control cells, suggesting that the expression of AFAP1L1 was not enough to produce distant metastasis in this animal model.

Discussion

Tumor type-specific molecular markers have been searched for in a variety of malignant tumors, in order to predict biological phenotype and/or serve as a target

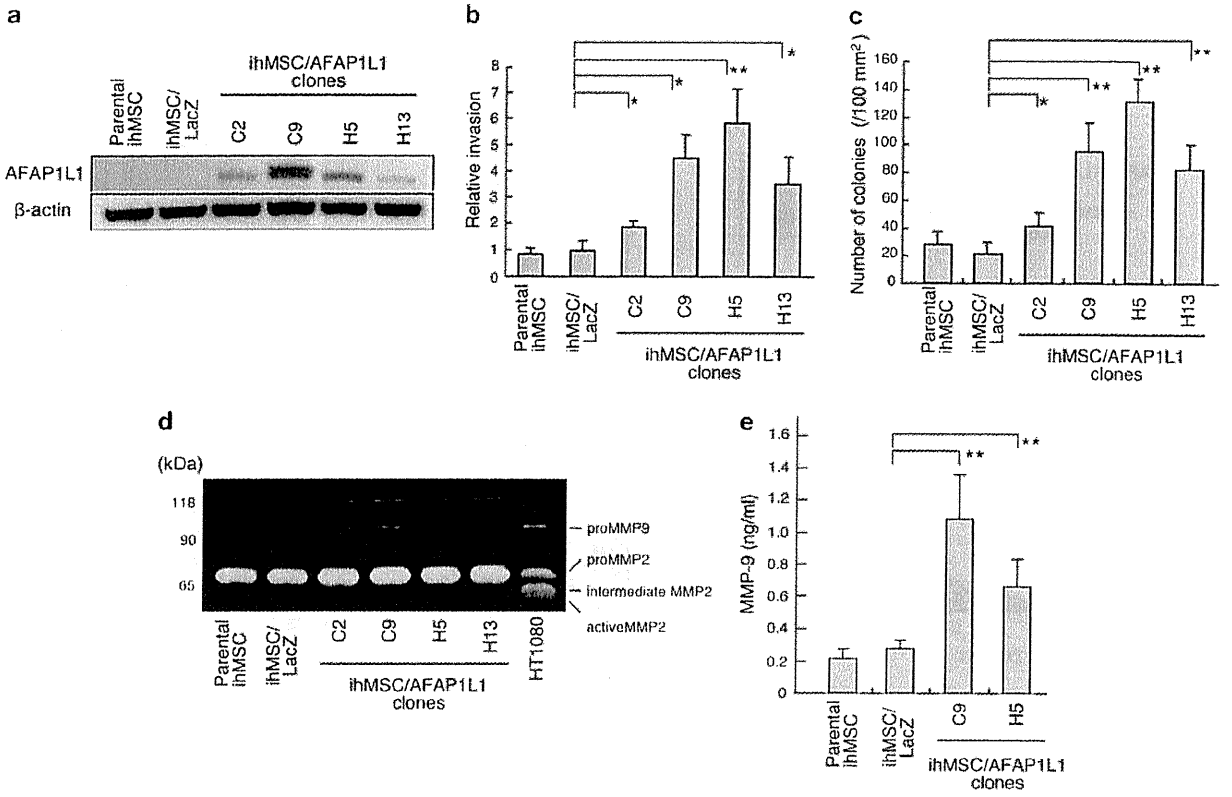

Figure 6 Upregulation of AFAP1L1 expression increased invasiveness and anchorage-independent growth of ihMSCs. (**a**) Western blotting of ihMSC clones stably expressing AFAP1L1. ihMSCs transduced with a LacZ-expressing lentivirus were used as a control. (**b**) Invasive ability of ihMSC clones transduced with AFAP1L1. Matrix invasiveness was calculated as described in materials and methods and demonstrated as fold change relative to LacZ-transduced cells. (**c**) Anchorage-independent growth of ihMSC clones transduced with AFAP1L1. (**d** and **e**) Production of MMP-9 in ihMSC clones transduced with AFAP1L1. Gelatin zymography (**d**) and enzyme-linked immunosorbent assay (**e**) demonstrated increased secretion of MMP-9 in ihMSC clones transduced with AFAP1L1. $^{**}P<0.01$; $^{*}P<0.05$.

for therapy. In the case of spindle cell sarcomas, however, the diversity and rarity of tumors have hampered such efforts. The importance of this study lies in having identified AFAP1L1 as a metastatic and a prognostic marker of spindle cell sarcomas, irrespective of pathological diagnosis. However, the significance of this gene in the development of distant metastasis should be carefully evaluated because our strategy focused on the contribution of single genes. Recently, two studies using large numbers of samples have been published relating to prognostic and therapeutic markers for soft tissue sarcomas. Barretina *et al.* (2010) performed an intensive analysis of 722 protein-coding and miRNA genes using a combination of DNA sequencing and a single-nucleotide polymorphism array and identified several tumor subtype-specific genetic alterations, some of which could be molecular targets for therapy. Chibon *et al.* (2010) identified a set of 67 genes on the basis of genomic and expression profiling and established a complexity index in sarcomas, which can predict the prognosis of patients. Among 67 genes, most were related to mitosis and chromosome management, and the *AFAP1L1* gene was not included.

Clinical results clearly demonstrated the association of AFAP1L1 with metastatic behavior of sarcomas in our cohorts, but the molecular mechanisms underlying this association are not yet clear. The results of knockdown and forced-expression experiments using sarcoma cell lines suggest that AFAP1L1 is involved in the process of invasion. Increased invasion of the matrix gel was confirmed in AFAP1L1-introduced ihMSC clones in association with an increase in excretion of MMP-9, a common feature of highly invasive malignant cells. We searched the ONCOMINE cancer array database (http://www.oncomine.org) and found a moderate correlation ($R^2 = 0.6964$) between AFAP1L1 and MMP-9 in glioblastomas (Sun *et al.*, 2006). We have no clear explanation of why we failed to find a clear association between the expression level of AFAP1L1 and that of MMP-9 in clinical samples (Supplementary Figure S1). This may be due to the multifactorial control of MMP-9 expression (St-Pierre *et al.*, 2004), and factors other than MMP-9 may be involved in the role of AFAP1L1 in tumor cell invasion. In this respect, it is intriguing that although the introduction of AFAP1L1 expression caused no change in growth profiles *in vitro*,

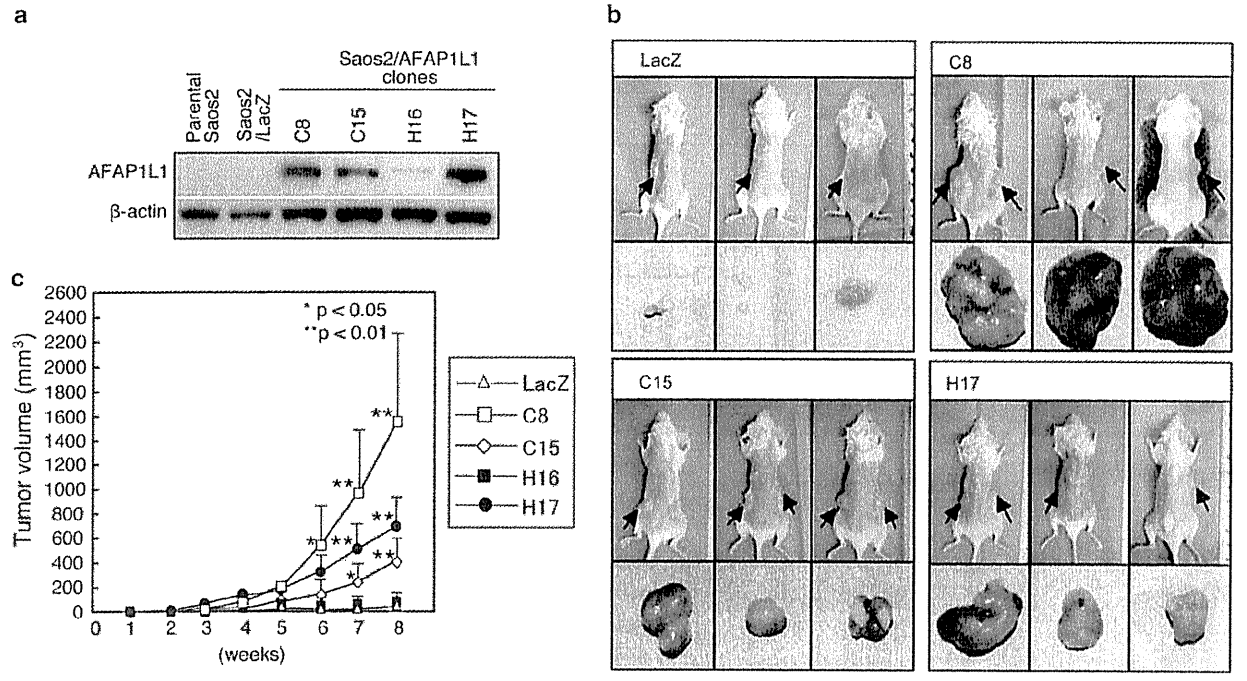

Figure 7 Acceleration of tumor growth by AFAP1L1 *in vivo*. (**a**) Western blotting of Saos2 clones stably expressing AFAP1L1. Saos2 cells transduced with a LacZ-expressing lentivirus were used as a control. (**b**) Macroscopic finding of tumors that developed in mice injected with AFAP1L1- or LacZ-transduced Saos2 clones. Tumors are indicated by arrows. (**c**) Growth curve of tumors shown in (**b**). $^{**}P<0.01$; $^{*}P<0.05$. Statistical examination was carried out by analysis of variance. Six mice were used for each cell clone.

the formation of tumor masses was accelerated *in vivo*. This suggested a role for AFAP1L1 at the interface between tumor cells and environments. Although the *AFAP1L1* gene was identified as a metastasis-associated gene from clinical data, we failed to find an association of metastasis with the expression of AFAP1L1 in experiments *in vivo*. The current experimental system using the subcutaneous inoculation of osteosarcomas cells may not be appropriate for evaluating the function of AFAP1L1.

AFAP1L1 is a paralogue of AFAP-110, which is an SH2/SH3-binding partner for Src (Flynn *et al.*, 1993; Guappone and Flynn, 1997; Qian *et al.*, 1998). AFAP-110 contains several protein-binding motifs at its amino terminus and functions as an adapter protein for actin filaments (Qian *et al.*, 2000; Baisden *et al.*, 2001b; Qian *et al.*, 2004). It is also required to control protein kinase Cα-mediated activation of c-Src and the subsequent formation of podosomes (Gatesman *et al.*, 2004). AFAP1L2, also known as XB130, is another paralogue of AFAP-110. AFAP1L2 associates with Src as well (Xu *et al.*, 2007) and is predominantly expressed in the thyroid (Lodyga *et al.*, 2009). AFAP1L2 cooperates with RET/PTC (rearranged in transformation/papillary thyroid carcinomas), a thyroid-specific tyrosine kinase, to increase phosphorylation of AKT, suggesting a role in thyroid cancer (Lodyga *et al.*, 2009). In addition, although AFAP1L2 has structural similarities to chicken AFAP-110 with which it was identified in a search of databases, it does not associate with actin filaments, suggesting a different role from that of AFAP-110 (Lodyga *et al.*, 2009). We have performed a series of experiments to examine the association of AFAP1L1 with actin filaments but found no definite evidence of one (data not shown). Although we speculate that AFAP1L1 acts as an adapter protein on the basis of its structural similarity to AFAP-110, AFAP1L1 functions in sarcoma cells via mechanisms distinct from those of AFAP-110, which may confer aggressive biological features.

Materials and methods

Clinical samples

Tumor samples were obtained at resection surgery in Kyoto University Hospital and preserved as described previously (Nagayama *et al.*, 2002). At least 90% of the viable cells in each specimen were identified as tumor cells. Primary hMSCs (hMSCs) were obtained and cultured by a method reported previously (Shibata *et al.*, 2007). All samples were approved for analysis by the ethics committee of the Faculty of Medicine, Kyoto University.

Cell lines

HS-SY-II was kindly provided by H Sonobe (Kochi University, Japan), SYO-1 by A Kawai (Okayama University, Japan), Fuji by S Tanaka (Hokkaido University, Japan), 1273/99 by O Larsson (Karolinska Institute, Sweden), NMS-2 (malignant peripheral nerve sheath tumor) by A Ogose (Niigata University, Japan) and GBS1 (MFH) by H Kanda (The Cancer Institute of the Japanese Foundation for Cancer

Research, Japan). ANOS, YaFuSS and an immortalized hMSC (ihMSC) line were established in our laboratory as described previously (Aoyama *et al.*, 2004; Ishibe *et al.*, 2005; Shima *et al.*, 2007). Other cell lines were purchased from American Type Culture Collection (Manassas, VA, USA) or Japanese Collection of Research Bioresources (JCRB) (Ibaraki, Japan). Cells were maintained in RPMI 1640 medium or Dulbecco's modified Eagle's medium (DMEM, Sigma-Aldrich, St Louis, MO, USA) with 10% fetal bovine serum (HyClone, Thermo Fisher Scientific Inc., Waltham, MA, USA) at 37 °C under 5% CO_2.

Production of anti-AFAP1L1 polyclonal antibody
The polyclonal antibody for AFAP1L1 was raised by immunizing rabbits with glutathione *S*-transferase-fused polypeptides corresponding to codon 35–113 of the human *AFAP1L1* gene and purified with standard protocols using affinity columns.

Immunohistochemical and immunocytochemical analyses
Immunohistochemical experiments using paraffin-embedded specimens of soft tissue sarcomas were performed as described previously (Kohno *et al.*, 2006). The anti-AFAP1L1 antibody was used at a concentration of 1 μg/ml. For immunocytochemistry, cells were fixed with 4% paraformaldehyde, permeabilized with 0.5% Triton X-100 and blocked with 1% bovine serum albumin in PBS. Slides were incubated with the anti-AFAP1L1 antibody or an anti-Flag M2 antibody (Sigma-Aldrich) overnight and then with a corresponding Alexa Fluor-conjugated secondary antibody (Invitrogen, Carlsbad, CA, USA). When indicated, rhodamine–phalloidin (Invitrogen) was used to stain actin fibers. Nuclei were stained with 4,6-diamidino-2-phenylindole. Cells were viewed with an IX81 (OLYMPUS, Tokyo, Japan) and photographed. The scoring was performed by two researchers without information on the clinical data for each sample.

Transient AFAP1L1 expression vectors
The coding region of the *AFAP1L1* gene was cloned into the pCAGGS vector (pCAG/AFAP1L1WT) tagged at the N-terminus with 3 × Flag. Transfection of these vectors was carried out using the Amaxa electroporation system (Amaxa Biosystems, Cologne, Germany) according to the manufacturer's instructions.

Lentiviral production
The BLOCK-iT Pol II miR RNAi Expression Vector Kit (Invitrogen) was used to knock down the *AFAP1L1* gene. Two oligonucleotides targeting AFAP1L1 (Hmi456004 and 456007, designated AFAP1L1 RNAi-1 and -2) and two control microRNAs that have no homology with mammalian gene sequences (designated control RNAi-1 and -2) were designed by and purchased from Invitrogen. They were annealed and ligated into the pcDNA6.2-GW/EmGFP-miR, in which microRNA expression was driven by a cytomegalovirus promoter with simultaneous expression of EmGFP. The cassette was subsequently cloned into pLenti6/V5-DEST, and cells were infected with supernatant containing microRNA lentiviruses (4.2×10^6 TU/ml) using the ViraPower Lentiviral Expression System (Invitrogen). These microRNA-transduced cells were prepared without drug selection or single-cell cloning. To generate cells stably expressing AFAP1L1, its gene was cloned into pLenti6/V5-DEST by a PCR-based method (pLenti6/AFAP1L1). As a control, a β-galactosidase gene-expressing vector (pLenti6/LacZ) was used. Cells were infected with these lentiviruses and selected with blasticidin (Invitrogen) for two weeks. Several clones of pLenti6/AFAP1L1-transduced cells were isolated by limiting dilution. pLenti6/LacZ-transduced control cells were used without cloning.

Western blot analyses
Western blot analyses were performed as described previously (Kohno *et al.*, 2006). Membranes were incubated overnight with the anti-AFAP1L1 (1:1000), anti-Flag M2 (1:4000; Sigma-Aldrich) or anti-β-actin (1:4000; Sigma-Aldrich) antibody.

Matrigel invasion assay
Cell suspensions (2.5×10^4) in 0.5 ml of DMEM without fetal bovine serum were placed in the upper chambers of 8 μm control cell culture inserts (BD Biosciences, Franklin Lakes, NJ, USA) or BioCoat matrigel invasion chambers (BD Biosciences), and 0.5 ml of DMEM containing 5% fetal bovine serum was placed in each lower chamber. After incubation for 22 h at 37 °C under 5% CO_2, cells on the upper surface of the membrane were mechanically removed. The membranes were fixed, and stained with 1% Toluidine blue. Cells were counted in five randomly chosen fields under a magnification of × 100. Cell invasiveness was calculated by dividing the number of cells invading through the matrigel membrane by the number invading the control insert.

Cell growth assay
Cells were seeded on 96-well plates at a density of 1000 per well in quadriplicate. The next day, cell viability was assessed by WST-8 using a Cell Counting Kit (DOJINDO, Kumamoto, Japan) every 24 h, according to the manufacturer's instructions.

Colony formation in soft agar
Cells (1×10^4) were suspended in DMEM containing 0.35% agarose and layered on a solidified 0.7% agarose layer in 60-mm tissue culture plates and cultured at 37 °C under 5% CO_2. After 4 weeks of incubation, p-iodonitrotetrazolium violet (Sigma-Aldrich) was added to count viable colonies.

Gelatin zymography
Gelatinolytic activity of the supernatant was analyzed as described elsewhere. Briefly, cells (4×10^5) were incubated with DMEM containing 10% fetal bovine serum for 24 h and then the medium was replaced with 0.5 ml of OptiMEM I (Invitrogen) containing 0.1% bovine serum albumin. After 16 h of incubation, the conditioned medium was analyzed on a 10% Tris–glycine gel containing 0.1% gelatin. The gel was treated with renaturating buffer for 30 min and with developing buffer for 12 h at 37 °C. Bands of gelatinolytic activity were visualized after staining the gels with 0.1% coomassie brilliant blue R-250 (Thermo Fisher Scientific Inc.) and then destaining. The digested bands were scanned by ChemiDocXRS (Bio-Rad Laboratories, Inc., Hercules, CA, USA).

Enzyme-linked immunosorbent assay
The expression of MMP-9 was quantified using a commercially available enzyme-linked immunosorbent assay system (Amersham matrix metalloproteinase-9 human biotrak ELISA system, GE Healthcare, Little Chalfont, UK) according to the manufacturer's instructions.

Animal experiments
All experiments with animals were approved by the Animal Research Committee (Graduate School of Medicine, Kyoto University) and conducted according to the Guidelines for Animal Experiments of Kyoto University. Cells (5×10^6)

suspended in 100 µl of PBS were injected subcutaneously into the hind flank region of female non-obese diabetic/Shi-*scid* Jic (non-obese diabetic/severe combined immunodeficient) mice at 5 weeks of age (Clea Japan, Tokyo, Japan). Tumor volumes were calculated using the formula: (length × width × height × 3.14)/6.

Reverse transcription and real-time qPCR

RNA extraction and reverse transcription were performed as described previously (Kohno *et al*., 2006). Real-time qPCR analyses were performed with the ABI PRISM 7700 Sequence Detection System (Applied Biosystems, Carlsbad, CA, USA). Taqman probes for AFAP1L1 (5′-GGCCCTTCCTCTGGGA CCCGGC-3′) and AFAP-110 (Taqman Gene Expression Assays Hs00222181_m1) were purchased from Applied Biosystems. 18S rRNA was also purchased from Applied Biosystems and used as an endogenous reference. Information on primers is available upon request.

Statistical analyses

Statistical analyses were performed using StatView software (SAS Institute Inc., Cary, NC, USA). Univariate and multivariate analyses were performed using Cox's proportional hazards model. The statistical significance of Kaplan–Meier curves was assessed by log-rank (Mantel–Cox) test. For comparisons of two individual data points, a two-sided Student's *t*-test was applied to assess statistical significance. An analysis of variance with *post hoc* testing was used for comparisons of more than three.

Conflict of interest

The authors declare no conflict of interest.

Acknowledgements

We thank Drs H Sonobe, A Kawai, S Tanaka, O Larsson, A Ogose, and H Kanda for providing cell lines, and T Tsunoda and S Miyano for data analyses. This work was supported by Grants-in-aid for Scientific Research from the Ministry of Education, Culture, Sports, Science and Technology.

References

Aoyama T, Okamoto T, Nagayama S, Nishijo K, Ishibe T, Yasura K *et al.* (2004). Methylation in the core-promoter region of the chondromodulin-I gene determines the cell-specific expression by regulating the binding of transcriptional activator, Sp3. *J Biol Chem* **279**: 28789–28797.

Baisden JM, Gatesman AS, Cherezova L, Jiang BH, Flynn DC. (2001b). The intrinsic ability of AFAP-110 to alter actin filament integrity is linked with its ability to also activate cellular tyrosine kinases. *Oncogene* **20**: 6607–6616.

Baisden JM, Qian Y, Zot HM, Flynn DC. (2001a). The actin filament-associated protein AFAP-110 is an adaptor protein that modulates changes in actin filament integrity. *Oncogene* **20**: 6435–6447.

Barretina J, Taylor BS, Banerji S, Ramos AH, Lagos-Quintana M, DeCarolis PL *et al.* (2010). Subtype-specific genomic alterations define new targets for soft-tissue sarcoma therapy. *Nat Genet* **42**: 715–721.

Chibon F, Lagarde P, Salas S, Pérot G, Brouste V, Tirode F *et al.* (2010). Validated prediction of clinical outcome in sarcomas and multiple types of cancer on the basis of a gene expression signature related to genome complexity. *Nat Med* **16**: 781–787.

Clark J, Rocques PJ, Crew AJ, Gill S, Shipley J, Chan AM *et al.* (1994). Identification of novel genes, SYT and SSX, involved in the t(X;18)(p11.2;q11.2) translocation found in human synovial sarcoma. *Nat Genet* **7**: 502–508.

Dorfleutner A, Stehlik C, Zhang J, Gallick GE, Flynn DC. (2007). AFAP-110 is required for actin stress fiber formation and cell adhesion in MDA-MB-231 breast cancer cells. *J Cell Physiol* **213**: 740–749.

Egeblad M, Werb Z. (2002). New functions for the matrix metalloproteinases in cancer progression. *Nat Rev Cancer* **2**: 161–174.

Francis P, Namlos HM, Muller C, Eden P, Fernebro J, Berner JM *et al.* (2007). Diagnostic and prognostic gene expression signatures in 177 soft tissue sarcomas: hypoxia-induced transcription profile signifies metastatic potential. *BMC Genomics* **8**: 73.

Fletcher CD, Gustafson P, Rydholm A, Willen H, Akerman M. (2001). Clinicopathologic re-evaluation of 100 malignant fibrous histiocytomas: prognostic relevance of subclassification. *J Clin Oncol* **19**: 3045–3050.

Fletcher CDM, Unni KK, Mertens F. (2002). *Pathology and Genetics of Tumours of Soft Tissue and Bones.* IARC Press: Lyon.

Flynn DC, Leu TH, Reynolds AB, Parsons JT. (1993). Identification and sequence analysis of cDNAs encoding a 110-kilodalton actin filament-associated pp60src substrate. *Mol Cell Biol* **13**: 7892–7900.

Gatesman A, Walker VG, Baisden JM, Weed SA, Flynn DC. (2004). Protein kinase Calpha activates c-Src and induces podosome formation via AFAP-110. *Mol Cell Biol* **24**: 7578–7597.

Guappone AC, Flynn DC. (1997). The integrity of the SH3 binding motif of AFAP-110 is required to facilitate tyrosine phosphorylation by, and stable complex formation with, Src. *Mol Cell Biochem* **175**: 243–252.

Helman LJ, Meltzer P. (2003). Mechanisms of sarcoma development. *Nat Rev Cancer* **3**: 685–694.

Ishibe T, Nakayama T, Aoyama T, Nakamura T, Toguchida J. (2008). Neuronal differentiation of synovial sarcoma and its therapeutic application. *Clin Orthop Relat Res* **466**: 2147–2155.

Ishibe T, Nakayama T, Okamoto T, Aoyama T, Nishijo K, Shibata KR *et al.* (2005). Disruption of fibroblast growth factor signal pathway inhibits the growth of synovial sarcomas: potential application of signal inhibitors to molecular target therapy. *Clin Cancer Res* **11**: 2702–2712.

Kanner SB, Reynolds AB, Vines RR, Parsons JT. (1990). Monoclonal antibodies to individual tyrosine-phosphorylated protein substrated of oncogene-encoded tyrosine kinases. *Proc Natl Acad Sci USA* **87**: 3328–3332.

Kohno Y, Okamoto T, Ishibe T, Nagayama S, Shima Y, Nishijo K *et al.* (2006). Expression of claudin7 is tightly associated with epithelial structures in synovial sarcomas and regulated by an Ets family transcription factor, ELF3. *J Biol Chem* **281**: 38941–38950.

Lee YF, John M, Falconer A, Edwards S, Clark J, Flohr P *et al.* (2004). A gene expression signature associated with metastatic outcome in human leiomyosarcomas. *Cancer Res* **64**: 7201–7204.

Lodyga M, De Falco V, Bai XH, Kapus A, Melillo RM, Santoro M *et al.* (2009). XB130, a tissue-specific adaptor protein that couples the RET/PTC oncogenic kinase to PI 3-kinase pathway. *Oncogene* **28**: 937–949.

Matushansky I, Hernando E, Socci ND, Mills JE, Matos TA, Edgar MA *et al.* (2007). Derivation of sarcomas from mesenchymal stem cells via inactivation of the Wnt pathway. *J Clin Invest* **117**: 3248–3257.

Nagayama S, Fukukawa C, Katagiri T, Okamoto T, Aoyama T, Oyaizu N *et al.* (2005). Therapeutic potential of antibodies against FZD 10, a cell-surface protein, for synovial sarcomas. *Oncogene* **24**: 6201–6212.

Nagayama S, Katagiri T, Tsunoda T, Hosaka T, Nakashima Y, Araki N *et al.* (2002). Genome-wide analysis of gene expression in synovial sarcomas using a cDNA microarray. *Cancer Res* **62**: 5859–5866.

Nakayama R, Nemoto T, Takahashi H, Ohta T, Kawai A, Seki K *et al.* (2007). Gene expression analysis of soft tissue sarcomas: characterization and reclassification of malignant fibrous histiocytoma. *Mod Pathol* **20**: 749–759.

Nielsen TO, West RB, Linn SC, Alter O, Knowling MA, O'Connell JX *et al.* (2002). Molecular characterization of soft tissue tumours: a gene expression study. *Lancet* **359**: 1301–1307.

Ottaiano A, De Chiara A, Fazioli F, Talamanca AA, Mori S, Botti G *et al.* (2005). Biological prognostic factors in adult soft tissue sarcomas. *Anticancer Res* **25**: 4519–4526.

Overall CM, Kleifeld O. (2006). Tumour microenvironment—opinion: validating matrix metalloproteinases as drug targets and anti-targets for cancer therapy. *Nat Rev Cancer* **6**: 227–239.

Qian Y, Baisden JM, Westin EH, Guappone AC, Koay TC, Flynn DC. (1998). Src can regulate carboxy terminal interactions with AFAP-110, which influence self-association, cell localization and actin filament integrity. *Oncogene* **16**: 2185–2195.

Qian Y, Baisden JM, Zot HG, Van Winkle WB, Flynn DC. (2000). The carboxy terminus of AFAP-110 modulates direct interactions with actin filaments and regulates its ability to alter actin filament integrity and induce lamellipodia formation. *Exp Cell Res* **255**: 102–113.

Qian Y, Gatesman AS, Baisden JM, Zot HG, Cherezova L, Qazi I *et al.* (2004). Analysis of the role of the leucine zipper motif in regulating the ability of AFAP-110 to alter actin filament integrity. *J Cell Biochem* **91**: 602–620.

Shibata KR, Aoyama T, Shima Y, Fukiage K, Otsuka S, Furu M *et al.* (2007). Expression of the p16INK4A gene is associated closely with senescence of human mesenchymal stem cells and is potentially silenced by DNA methylation during *in vitro* expansion. *Stem Cells* **25**: 2371–2382.

Shima Y, Okamoto T, Aoyama T, Yasura K, Ishibe T, Nishijo K *et al.* (2007). *In vitro* transformation of mesenchymal stem cells by oncogenic H-rasVal12. *Biochem Biophys Res Commun* **353**: 60–66.

St-Pierre Y, Couillard J, Van Themsche C. (2004). Regulation of MMP-9 gene expression for the development of novel molecular targets against cancer and inflammatory diseases. *Expert Opin Ther Targets* **8**: 473–489.

Sun L, Hui AM, Su Q, Vortmeyer A, Kotliarov Y, Pastorino S *et al.* (2006). Neuronal and glioma-derived stem cell factor induces angiogenesis within the brain. *Cancer Cell* **9**: 287–300.

Toguchida J, Nakayama T. (2009). Molecular genetics of sarcomas: applications to diagnoses and therapy. *Cancer Sci* **100**: 1573–1580.

Toguchida J, Yamaguchi T, Ritchie B, Beauchamp RL, Dayton SH, Herrera GE *et al.* (1992). Mutation spectrum of the p53 gene in bone and soft tissue sarcomas. *Cancer Res* **52**: 6194–6199.

Wadayama B, Toguchida J, Shimizu T, Ishizaki K, Sasaki MS, Kotoura Y *et al.* (1994). Mutation spectrum of the retinoblastoma gene in osteosarcomas. *Cancer Res* **54**: 3042–3048.

Xu J, Bai XH, Lodyga M, Han B, Xiao H, Keshavjee S *et al.* (2007). XB130, a novel adaptor protein for signal transduction. *J Biol Chem* **282**: 16401–16412.

Zhang J, Park SI, Artime MC, Summy JM, Shah AN, Bomser JA *et al.* (2007). AFAP-110 is overexpressed in prostate cancer and contributes to tumorigenic growth by regulating focal contacts. *J Clin Invest* **117**: 2962–2973.

Supplementary Information accompanies the paper on the Oncogene website (http://www.nature.com/onc)

整・災外 54：1159−1170，2011

特集 炎症など悪性骨・軟部腫瘍と見まちがう疾患 ―診断のポイント

骨組織球症

―臨床・画像上の特徴と悪性腫瘍との鑑別―

保坂正美[*1] 羽鳥正仁[*2] 常陸 真[*3]
綿貫宗則[*1] 相沢俊峰[*1] 井樋栄二[*1]

要旨：当科で経験した骨発生ランゲルハンス細胞組織球症（骨組織球症）9例について臨床像，血液所見，および画像所見を検討した。初発症状は疼痛が多く，腫脹は1例にとどまった。血液所見では白血球値は正常から高値，CRPは正常から軽度上昇を示した。単純X線像およびCTでは辺縁骨硬化像とendosteal scallopingが多くみられた。MRIでは骨内および周囲軟部組織の浮腫性変化が多くみられたものの，骨外に大きく膨隆するような腫瘤性病巣は確認されなかった。初発症状として腫脹が軽微であること，血液・生化学所見で炎症反応が比較的軽度であること，画像上，病期による違いが大きく，病巣周囲の浮腫が顕著であるが骨外へ進展する大きな腫瘤性病変がみられないことが悪性骨腫瘍，特にユーイング肉腫との鑑別において重要な点と考えられた。本疾患を炎症性肉芽腫疾患の一つとして新たに捉え直すことが，診断へのアプローチとして重要と思われた。

Ⅰ．歴史的背景

ドイツの外科医であるPaul Wilhelm Heinrich Langerhans（1847〜1888）は，1868年に上皮に存在する非色素性樹状細胞を世界で初めて報告した（原題 Über die Nerven der menschlichen Haut，英語名：On the Nerves of the Human Skin）。この細胞が現在ランゲルハンス細胞と呼ばれている[1)2)]。1893年Handは口渇，多尿症，眼球突出，肝脾腫を呈する3歳の男児の報告を行った。これがランゲルハンス細胞組織球症（以下，LCH）についての最も信頼性の高い最初の報告である。原因は当初，結核と考えられていた。1953年Lichtensteinが好酸球性肉芽腫症，Hand-Schüller-Christian病，Letterer-Siwe病などの組織球の浸潤・増殖を組織学的特徴とする疾患をHistiocytosis Xと名づけた[3)4)]。1987年に国際組織球学会が，微細形態および免疫組織化学的研究を踏まえ，組織球症を3つに分類した[5)6)]。Histiocytosis Xは，このときにLangerhans cell histiocytosis（LCH）と正式に呼称されるようになった。

*1) Masami HOSAKA et al，東北大学大学院医学系研究科，整形外科学
*2) Masahito HATORI，東北公済病院，整形外科
*3) Shin HITACHI，東北大学病院，放射線診断科

Langerhans cell histiocytosis of bone；clinical and radiological aspects and differential points from malignant tumor

Key words：Langerhans cell histiocytosis of bone, Eosinophilic granuloma of bone, Ewing sarcoma

Ⅱ．LCHの分類

LCHの臨床分類は現在，主に病巣の広がりによってなされている[6)〜8)]（表1）。本稿ではLCHのうち単一臓器発生（SS-LCH）のうち骨に限局し

表 1　LCH の分類[6)~8)]

1．単一臓器発生（single-system disease：SS-LCH）
　(1) 単発型（single site, unifocal）
　　骨，リンパ節，肺など単一臓器に単独に発生する。
　(2) 多発型（multiple site, multifocal）
　　骨やリンパ節などに複数発生する。

2．多臓器発生（multi-system disease：MS-LCH）
　(1) 臓器不全を伴わないもの
　(2) 臓器不全を伴うもの
　　低リスク群：皮膚，骨，リンパ節
　　高リスク群：肺，肝，脾，造血器

表 2　X 線像上の発育速度の分類[16)17)]

Grade ⅠA：Geographic lesion with sclerotic margin
Grade ⅠB：Geographic lesions with sharp nonsclerotic margin
Grade ⅠC：Geographic lesions with poorly defined margin
Grade Ⅱ　：Geographic lesions with moth-eaten or permeative component
Grade ⅢA：Moth-eaten component
Grade ⅢB：Permeative component

表 3　当科の骨組織球症症例（臨床所見）

症例	年齢（歳）	性	部位	生検方法	生検までの期間	初発症状	局所所見
1	2	男	橈骨	open	2 週間	夜間痛（夜泣き）	硬性腫脹（発赤，発熱なし）
2	2	男	腸骨	針（CT ガイド下），open	1 カ月	跛行	特になし
3	4	男	鎖骨	open	1 カ月	腫脹	腫脹
4	4	男	腸骨（臼蓋）	針（X 線透視下）	2 カ月	跛行	圧痛
5	6	男	腸骨（臼蓋）	open	3 カ月	跛行，疼痛（安静，動作時）	Patrick（＋）
6	9	男	L5	針（X 線透視下）	5 カ月	疼痛	圧痛，側弯
7	28	男	腸骨	針（CT ガイド下）	2 カ月	疼痛	圧痛
8	28	男	T1	針（X 線透視下）	1 カ月	疼痛	圧痛，上肢しびれ感
9	33	男	恥骨	針（CT ガイド下）	3 カ月	疼痛	圧痛（違和感程度）

表 4　当科の骨組織球症症例（血液・生化学所見）

症例	年齢（歳）	部位	白血球数	好酸球（%）	CRP
1	2	橈骨	10,600	記録なし	0.9
2	2	腸骨	11,460	2.8	0.23
3	4	鎖骨	14,200	4.9	0.87
4	4	腸骨（臼蓋）	8,520	記録なし	0.3 以下
5	6	腸骨（臼蓋）	7,800	4.7	0.58
6	9	L5	5,300	2	0.2
7	28	腸骨	7,800	1	0.6
8	28	T1	6,600	1	0.5
9	33	恥骨	8,100	4	0.1 以下

て発生する症例について骨発生ランゲルハンス細胞組織球症（以下，骨組織球症）として表記する。これは従来より呼称されている（骨）好酸球性肉芽腫とほぼ合致する。

表 5　当科の骨組織球症症例（画像所見）

例	年齢（歳）	部位	単純 X 線/CT				MRI		
			骨皮質破壊	骨膜反応	Endosteal scalloping	辺縁硬化	髄内浮腫	骨外浮腫	骨外膨隆
1	2	橈骨	○	○	○	○	○	○	×
2	2	腸骨	○	×	×	×	○	○	○（一部）
3	4	鎖骨	○	○	○	○	○	○	○
4	4	腸骨（臼蓋）	○	×	○（一部）	○（一部）	○	×	×
5	6	腸骨（臼蓋）	○	×	×	○	○	○	×
6	9	L5	○	×	○	○	○	○	×
7	28	腸骨	○	×	×	○	○	○	○（一部）
8	28	T1	○	×	○（一部）	○（一部）	○	○	○
9	33	恥骨	○	×	○	○（一部）	○	×	×

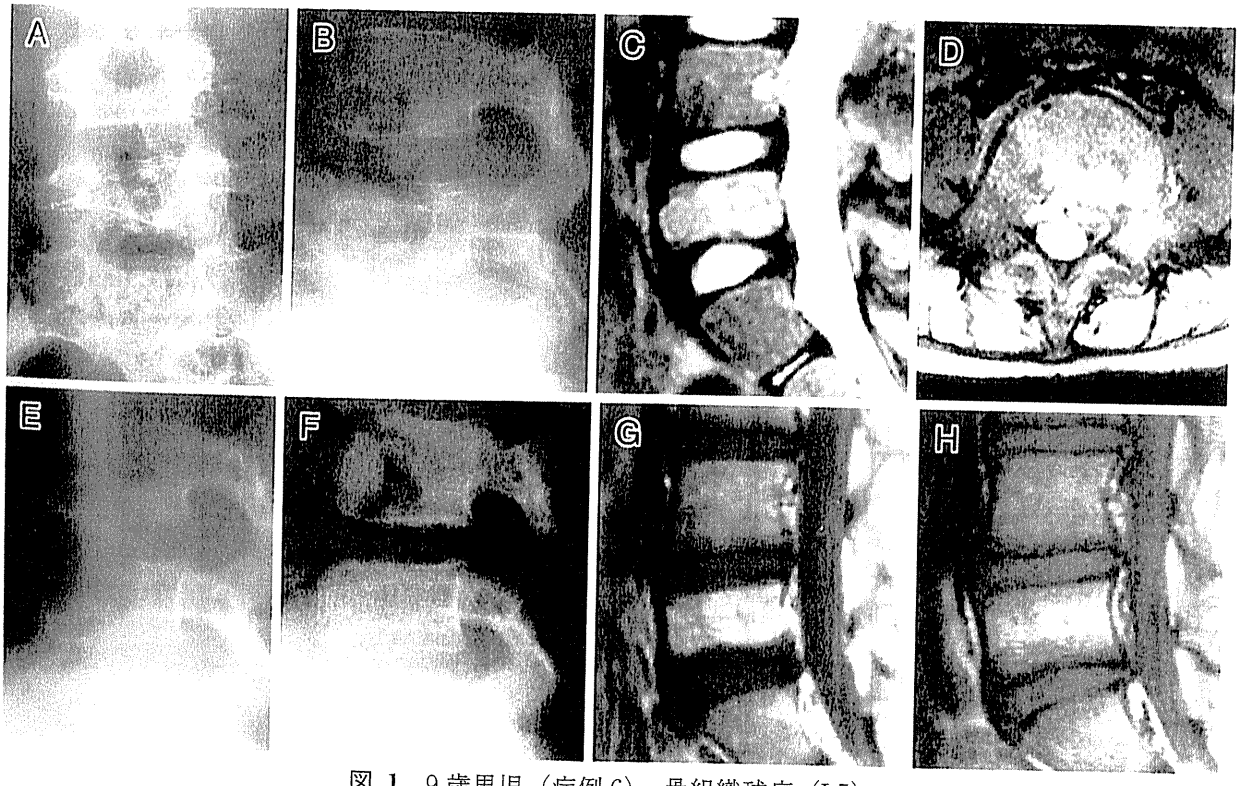

図 1　9 歳男児（症例 6），骨組織球症（L5）
A　初診時単純 X 線正面像。L5 椎体左側の圧潰がみられる。
B　同側面像。椎体の骨溶解像がみられる。
C　初診時 MRI（T2 強調矢状断）。病変は骨髄より高信号である。
D　同 MRI（T2 強調水平断）。骨外病巣は明らかではない。
E　10 カ月後の単純 X 線側面像。
F　3 年後の単純 X 線側面像。椎体の圧潰は徐々に改善した。
G　10 カ月後の MRI（T1 脂肪抑制造影後矢状断）。骨内に造影効果がみられる。
H　3 年後の MRI（T1 脂肪抑制造影後矢状断）。造影効果が減弱した。

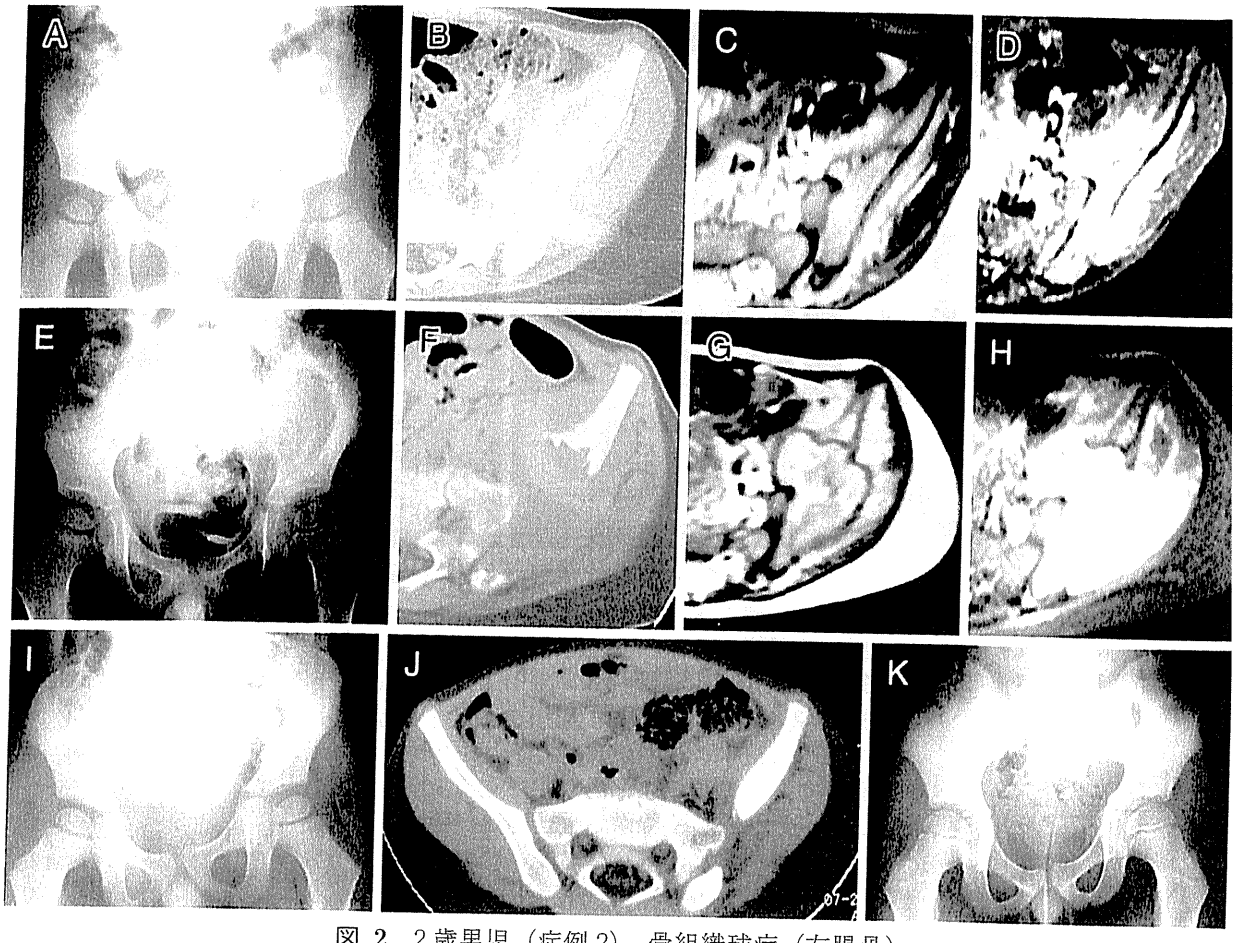

図 2　2歳男児（症例2），骨組織球症（左腸骨）

A～D　初回生検時（初発より1カ月後）。
A　単純X線正面像。左腸骨内側，仙腸関節部の辺縁不明瞭な骨透亮像がみられる。
B　単純CT。軟骨下骨の消失がみられる。骨膜反応や周囲の骨硬化像は明らかでない。
C　MRI（T2強調水平断）。髄内および骨外のびまん性の信号の上昇がみられる。仙腸関節部前方で骨外進展がみられる。
D　MRI（T1強調脂肪抑制造影像）。髄内および骨外軟部組織のびまん性造影効果がみられる。
E～H　第2回生検時（初回生検より1カ月後）
E　単純X線正面像。左腸骨内側の骨透亮像の拡大がみられるが，辺縁の骨硬化像が出現している。
F　CT。病巣の外側部で周囲の骨硬化とendosteal scallopingが捉えられる。
G　MRI（T2強調水平断）。髄内より骨外へ病巣の拡大がみられる。
H　MRI（T1強調脂肪抑制造影後）。髄内および骨外のびまん性の造影効果がみられる。
I　第2回生検7カ月後単純X線正面像。辺縁の骨硬化が進行している。
J　7カ月後単純CT。骨の再生がみられるが変形が残存している。
K　4年後単純X線像。変形が残存しているが特に愁訴はみられない。

Ⅲ．LCHの病態

LCHは上皮に存在する正常樹状細胞と同様の形態を有する組織球であるランゲルハンス細胞の異常増殖と播種が特徴である[2]。ランゲルハンス細胞は上皮，リンパ節，胸腺，消化管，呼吸器および子宮頚部の粘膜上皮に存在し，正常な樹状胞の表面抗原を多数有する抗原提示細胞である[2)9)]。免疫組織化学的にはHLA-DR，CD1-a S100，Fc-recepter陽性，Lysozyme陰性であ

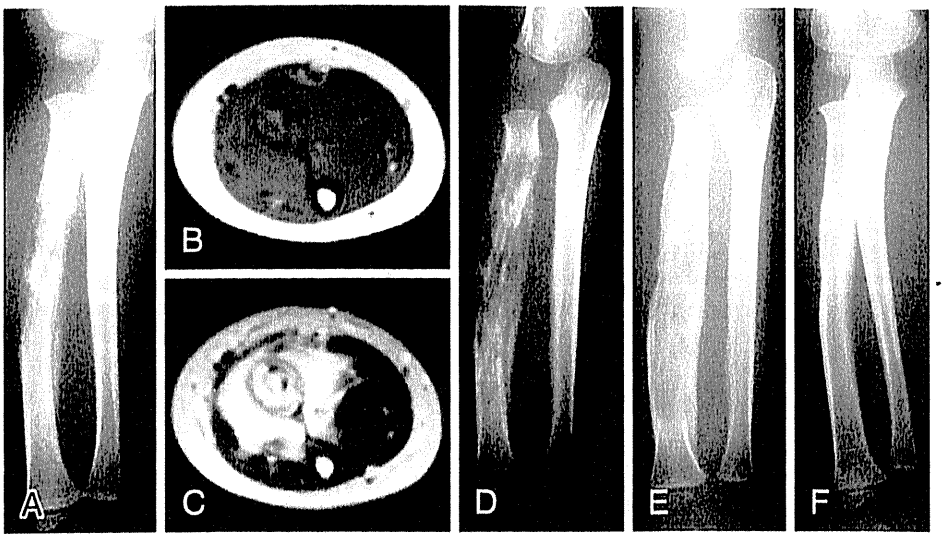

図 3　症例 1（2 歳男児），骨組織球症（右橈骨）

A　初診時単純 X 線正面像。虫喰い状陰影，骨膜反応がみられる。辺縁が比較的明瞭である。
B　初診時 MRI T1 強調（水平断）。髄内信号の低下がみられる。
C　初診時 MRI（T2 強調）。骨外の信号上昇がみられる。
D　生検時（初診より 1 週後，発症より 2 週後）の単純 X 線像。虫喰い陰影とともに周囲の硬化性変化や scalloping がみられる。
E　1 カ月後の単純 X 線像。骨透亮像が軽快している。
F　1 年後の単純 X 線像。骨透亮像は消失している。

細胞内小器官である Birbeck 顆粒が電子顕微鏡で観察される[9)10)]。LCH は現在，CD1-a 陽性の樹状細胞であるランゲルハンス細胞の制御困難なクローン性増殖により特色づけられる組織球性疾患として位置づけられている[10)11)]。LCH は歴史的に腫瘍説，非腫瘍説（結核などの感染症を含め）について議論がなされているが，現在のところ真の腫瘍ではなく，ランゲルハンス細胞から放出されるサイトカインによる急性から慢性の炎症性肉芽腫と理解される。

Ⅳ. 臨床所見

骨組織球症の臨床症状としては Arckader ら[12)]によると，小児において疼痛（79%）が最も多く，特に脊椎症例の 94%は疼痛を伴っていた。次いで腫脹（15%），歩容異常（11%），知覚異常（5%），ほかに斜頸，高熱，咳，発疹，尿崩症，病的骨折などを呈した。病的骨折はまれとされる[13)]。血液所見の特徴としては血沈の軽度亢進，まれに末梢血好酸球の増加がみられるとされる[13)]。

Ⅴ. 画像所見

骨組織球症の画像所見は多様であり，部位および病期によって大きく異なることが特徴である[14)15)]。長管骨においては骨幹部に多発する。骨幹端の発生は少ない。まれに骨端線を越え骨端に至る。骨端の発生はまれである。多くは楕円形の骨溶解像を呈し，ゆっくりした進行（Grade ⅠA～Grade Ⅱ：辺縁明瞭な地図状陰影～虫喰い状または浸潤部位を含む地図状陰影）を示すが，急速な骨破壊（Grade Ⅲ：虫喰いまたは浸潤性）を示す場合もある[16)17)]（表 2）。Endosteal scalloping，cortical thinning，intracortical tunneling，髄腔の拡大が一般的な X 線像である。多発小病巣が合体したり重なり合うと，hole-within-a-hole appearance と呼ばれる[18)]。頭蓋骨においては直径 1～4 cm の円形から類円形の複数の溶骨性陰影がみられることが多い。辺縁は明瞭であり，